AD_____

Award Number:

W81XWH-07-1-0601

TITLE:

Early Diagnosis, Treatment, and Care of Cancer Patients”

PRINCIPAL INVESTIGATOR:

Richard Fisher, MD

CONTRACTING ORGANIZATION:

University of Rochester
Rochester, NY 14627

REPORT DATE:
September 2010

TYPE OF REPORT: **Annual**

PREPARED FOR: U.S. Army Medical Research and Materiel Command
Fort Detrick, Maryland 21702-5012

DISTRIBUTION STATEMENT:

X Approved for public release; distribution unlimited

REPORT DOCUMENTATION PAGE

Form Approved
OMB No. 0704-0188

1. REPORT DATE *(DD-MM-YYYY)*	2. REPORT TYPE	3. DATES COVERED *(From - To)*
01-09-2010	Annual	1 SEP 2009 - 31 AUG 2010

4. TITLE AND SUBTITLE
Early Diagnosis, Treatment, and Care of Cancer Patients

5a. CONTRACT NUMBER

5b. GRANT NUMBER
W81XWH-07-1-0601

5c. PROGRAM ELEMENT NUMBER

6. AUTHOR(S)
Craig T. Jordan

Richard I. Fisher

E-Mail: Richard_Fisher@urmc.rochester.edu

5d. PROJECT NUMBER

5e. TASK NUMBER

5f. WORK UNIT NUMBER

7. PERFORMING ORGANIZATION NAME(S) AND ADDRESS(ES)

University of Rochester

Rochester, NY 14642

8. PERFORMING ORGANIZATION REPORT NUMBER

9. SPONSORING / MONITORING AGENCY NAME(S) AND ADDRESS(ES)
US Army Medical Research
And Material Command
Fort Detrick, MD 21702-5012

10. SPONSOR/MONITOR'S ACRONYM(S)

11. SPONSOR/MONITOR'S REPORT NUMBER(S)

12. DISTRIBUTION / AVAILABILITY STATEMENT

Approved for public release; distribution unlimited

13. SUPPLEMENTARY NOTES

14. ABSTRACT

This grant program encompasses two complimentary projects. The hypothesis that leukemia can be treated effectively by inhibition of putative cancer stem cells will be tested in project #1. This will be done by application of inhibitors of stem cells as a novel approach for eradication of leukemia tumor cells. Parthenolide (PTL)-based drugs and related drugs that inhibit nuclear factor kappa B (NF-κB) will be used. The effects of these drugs will also be tested on normal hematopoietic cells. In project 2, studies will investigate how standard therapies effect normal CNS stem cells, and will attempt to develop less toxic regimens for the treatment of brain cancers. To this end, studies will determine whether parthenolide or related drugs cause CNS damage in animals treated with these substances, and will assess whether parthenolide can function as a chemosensitizing agent for various conventional chemotherapy drugs.

15. SUBJECT TERMS
leukemia, stem cell, cancer, parthenolide, oligodendrocyte, progenitor

16. SECURITY CLASSIFICATION OF: unclassified			17. LIMITATION OF ABSTRACT	18. NUMBER OF PAGES	19a. NAME OF RESPONSIBLE PERSON
a. REPORT U	b. ABSTRACT U	c. THIS PAGE U	UU	24	USAMRMC
					19b. TELEPHONE NUMBER *(include area code)*

Table of Contents

Introduction

This grant is comprised of two complementary projects. For the purposes of this report, progress for each project will be described separately below.

Body

Project 1

The objective of this project is to develop a novel therapeutic agent that specifically targets human leukemia stem cells (LSC). While the concept of a critical leukemia stem cell in myeloid disease has been postulated for over three decades, to date no therapeutic agent has been identified that specifically and preferentially ablates LSC in vivo. Thus, the central premise of this grant is that direct targeting of LSC will yield more effective therapy for leukemia. Previously, we demonstrated that parthenolide (PTL) is highly cytotoxic to LSC in vitro, but does not significantly affect normal hematopoietic stem cells (HSC). However, solubility of PTL is limiting; thus we have generated a PTL analog, dimethyl amino parthenolide (DMAPT), that is much more soluble in water and retains the anti-leukemic activity of PTL. Using this agent, the tasks below were specified:

SOW task #1: To demonstrate that a parthenolide analog can be used for preclinical and clinical applications related to treatment of chronic leukemia (Months 1-36).

Progress: As noted in previous reports, there is substantial evidence that parthenolide-based drugs can be effective for the eradication of leukemic cells. Further, DMAPT has progressed to clinical trials (ongoing) and represents an intriguing “first in class” agent. However, despite the development of DMAPT, we believe there is still significant opportunity for further pharmacological improvement of parthenolide-based compounds. DMAPT has a relatively short in vivo half-life (approximately two hours) which may limit its activity. Moreover, the design of this molecule does not readily afford opportunities to develop tissue-targeting strategies due to stability problems associated with drug formulation. This is related to the ability of the drug to undergo reverse Michael deamination reactions to generate parthenolide. Thus, we have continued to investigate ways to both improve the biological activity of PTL and create novel pharmacological agents with drug-like characteristics that can be formulated as oral dosage forms. In performing such studies, one PTL analog that was synthesized via selenium oxide oxidation was a C10 hydroxymethyl derivative. Notably, hydroxylation of the C10 methyl group of PTL resulted in the concomitant conversion of the geometry of the C9-C10 double bond from *trans* to *cis* (Figure 1). The resulting product, a hydroxymethyl 1(10)-*cis*-parthenolide analog, has previously been reported as melampomagnolide B (MMB) (El-Feraly, 1984). This compound is of great interest to us for two reasons. First, the anti-

leukemia activity of MMB is excellent, and indistinguishable from PTL (Figure 2). Second, as a functionalized analog of PTL, the MMB molecule allows the synthesis of conjugated analogs that retain biological activity. For example, as a laboratory tool, we created a biotinylated analog of MMB via conjugation at the allylic hydroxyl group, and used this reagent to identify MMB target proteins in

Fig. 1

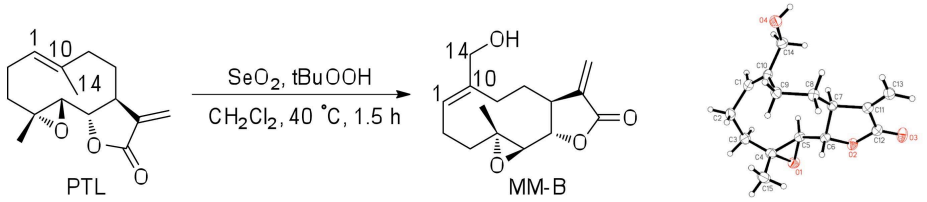

AML cells (Figure 3). This approach has been extremely useful in better understanding the underlying mechanisms by which anti-leukemia (and anti-LSC) activity is achieved. Unfortunately, MMB does not possess good drug-like properties for oral administration, as determined by the Lipinsky's "rule of five" (Lipinski et al., 1997), and its physicochemical properties would have to be modified considerably to meet these requirements. Therefore, we have developed a plan to use MMB as an lead compound from which to synthesize a new family of novel *prodrugs* in which the prodrug moiety has been conjugated to the allylic hydroxyl function, and which have been designed to improve the oral bioavailability and drugability of MMB. A prodrug is defined as pharmacologically inactive molecule that is converted into an active drug entity via metabolic biotransformation. The utility of prodrugs and their specific design, usually address a particular problem or flaw in the drug-like characteristics of the parent active compound. Such problems may include poor aqueous solubility, poor absorption and distribution, rapid first-pass metabolism, instability, and formulation problems. For prodrugs that are to be utilized as oral dosage forms, the prodrug-to-drug conversion should occur after absorption from the gastrointestinal tract. Thus, the prodrug should be designed to possess optimal drug absorption characteristics through the gastrointestinal mucosa into

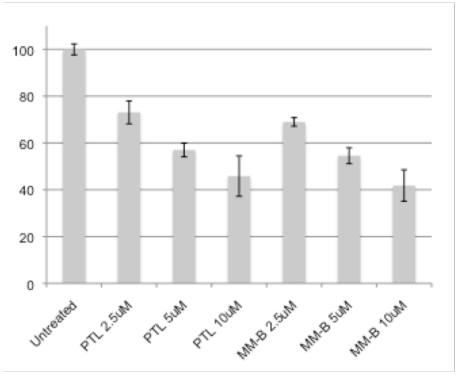

Figure 2: PTL vs. MM-B activity
Viability of primary AML specimens treated for 18 hours with PTL or MM-B.

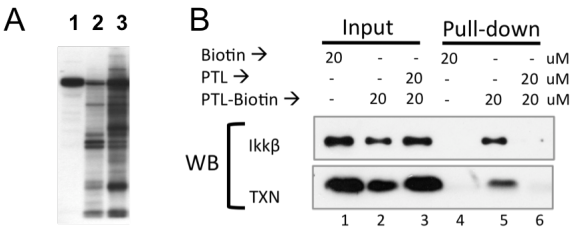

Figure 3: Biochemical studies with MM-B-biotin
A) Western blot analysis using MM-B-Biotin as probe. Lane 1 = ctrl, 2 = normal cells, 3 = AML cells. B) Primary AML cells were treated with PTL-biotin for 6 hours followed by lysis and biochemical pull-downs using streptavidin conjugated agarose beads. Controls include cells incubated with biotin alone, or preincubated with native PTL prior to the addition of PTL-biotin (i.e. competitive binding studies). Lysates were analyzed by western blot (WB) for the presence of IKK or thioredoxin (TXN). Lanes 1-3 labeled "input" represent whole cell lysates for each condition. Lanes 4-6 labeled "pull-down" are the material that was bound to streptavidin beads. No pull-down is observed with biotin alone (lane 4). Both proteins are bound by PTL-biotin (lane 5). Pre-incubation with PTL competes the PTL-biotin interaction (lane 6).

plasma, and should exhibit maximal stability while in the gastrointestinal tract. Once in the plasma, the prodrug should undergo facile enzymatic cleavage to liberate the active drug molecule. Such characteristics can be achieved by appropriate design of the prodrug moiety. Thus, we believe that the development of novel MMB prodrugs represents a substantially improvement in our overall strategy to employ parthenolide-based agents for the treatment of leukemia.

Please note: A more detailed description of the synthesis and characterization of MMB is provided in Appendix A.

SOW task #2: To demonstrate that a parthenolide analog can function as a chemosensitizing agent to enhance ablation of chronic leukemia cells (Months 37-60).

Progress: Not started yet

Project 2

The primary goal of this project is to investigate how standard therapies effect normal CNS stem cells and to develop less toxic regimens for the treatment of cancer:

SOW task #1: To determine whether parthenolide or parthenolide analogs cause CNS damage in animals treated with these substances, and to determine whether parthenolide or parthenolide analogs enhance the damage caused by cytarabine. (Months 1-24)

Progress:

SOW task #2: Demonstrate that mice in which purified cells are more oxidized in vitro will exhibit more extensive damage from cytarabine, parthenolide (or parthenolide analogs) or the combination of these agents, than those in which purified cells are intrinsically more reduced (Months 25-48).

Progress: Not started yet.

SOW task #3: To initiate identification of potential prognostic indicators to detect individuals at greater risk for adverse side effects of therapy with cytarabine, parthenolide (or parthenolide analogs) or the combination of these agents, and

begin testing to provide proof of principle for protective strategies that involve administration of N-acetyl-L-cysteine (alone or in combination with Vitamins E and/or C) as an anti-oxidant to protect against oxidative damage (Months 49-60).

Progress: Not started yet.

Key Research Accomplishments

Development of parthenolide-based molecule (melampomagnolide B) which provides a foundation for novel prodrugs.

Conclusion

MMB-based prodrugs represent a promising new line of agents towards the overall goal of developing improved therapies for leukemia.

Reportable outcomes

1. Hassane DC, Sen S, Minhajuddin M, Rossi RM, Corbett CA, Balys M, Wei L, Crooks PA, Guzman ML, and Jordan CT. Chemical Genomic Screening Reveals Synergism between Parthenolide and Inhibitors of the PI-3 Kinase and mTOR Pathways. *Blood*, 2010 Dec 23;116(26):5983-90. PMID: 20889920

2. Nasim S, Pei S, Hagen FK, Jordan CT, and Crooks PA. Melampomagnolide B: a new antileukemic sesquiterpene. *Bioorg and Med Chem*, 2011, in press (available online January 6th, 2011).

3. Konopleva M.Y., and Jordan C.T. (2011) Leukemia Stem Cells and Microenvironment: Biology and Therapeutic Targeting. J Clin Oncol. 2011 Jan 10 [Epub ahead of print]. PMID: 21220598.

4. Becker, M.W., and Jordan, C.T. (2011) Leukemia stem cells in 2010: Current understanding and future directions. Blood Rev. 2011 Jan 7. [Epub ahead of print]. PMID: 2121651

Appendices

Appendix A:

1. Nasim S, Pei S, Hagen FK, Jordan CT, and Crooks PA. Melampomagnolide B: a new antileukemic sesquiterpene. *Bioorg and Med Chem*, 2011, in press (available online January 6th, 2011).

Project 2

The primary goal of this project is to investigate how standard therapies effect normal CNS stem cells and to develop less toxic regimens for the treatment of cancer:

SOW task #1: To determine whether parthenolide or parthenolide analogs cause CNS damage in animals treated with these substances, and to determine whether parthenolide or parthenolide analogs enhance the damage caused by cytarabine. (Months 1-24)

Our work on this task was described in last year's project report, with detailed data presented for our new findings on toxicity. In brief, we have found that most cancer treatment regimens that we examine are toxic for progenitor cells and oligodendrocytes of the CNS. At this stage, we have demonstrated toxicity (both in vitro and in vivo) for BCNU, cisplatin, cyclophasphamide, vincristine, cytarabine, 5-fluorouracil and tamoxifen. We also have examined multiple regions of the CNS.

At this stage, and for reasons described below in relation to task 3, we can say that this task is effectively completed with the demonstration that the toxicity that we have identified is a problem that permeates through the world of cancer treatment and that it affects multiple subsystems within the CNS.

SOW task #2: Demonstrate that mice in which purified cells are more oxidized in vitro will exhibit more extensive damage from cytarabine, parthenolide (or parthenolide analogs) or the combination of these agents, than those in which purified cells are intrinsically more reduced (Months 25-48).

SOW task #3: To initiate identification of potential prognostic indicators to detect individuals at greater risk for adverse side effects of therapy with cytarabine, parthenolide (or parthenolide analogs) or the combination of these agents, and begin testing to provide proof of principle for protective strategies that involve administration of N-acetyl-L-cysteine (alone or in combination with Vitamins E and/or C) as an anti-oxidant to protect against oxidative damage (Months 49-60).

Task 2 and 3 are considered together for two reasons. First, the interest in oxidative state that applies to both of these tasks links them together functionally. Second, the discoveries that are the focus of this year's report have been so exciting that we have changed the time line of experimentation in order to complete the studies that we will describe.

In respect to our analysis of the importance of oxidative biology in understanding and predicting vulnerability, we have made important strides. We are still testing key hypotheses in this arena, however, and will report on this in a comprehensive manner next year.

This year our focus is necessarily on protection, due to the progress we have made.

It is clear that treatment with chemotherapy is going to remain the mainstay of cancer treatment for many years to come, thus making the development of strategies for protecting against neurological damage of central importance. This is a considerable challenge, particularly as virtually nothing is known about whether such protection is even conceivable. Is damage to the central nervous system inevitable for a subset of individuals treated with chemotherapy or is it possible to prevent such damage? As multiple CNS cell types are damaged by many different chemotherapeutic agents, is it is possible to identify protective approaches that are similarly

broad in their utility. Or will multiple protective strategies be required in order to rescue different cell types? Moreover, as both acute and delayed damage occurs, it is necessary to find means of protecting normal tissue that similarly protect from both acute and delayed damage. But attempts to rescue the cells of the CNS from this type of damage represents a new field of discovery, and it is not known whether any single agents exist that are capable of preventing damage to multiple different cell types or can provide protection at both early and late time points.

We now have found that erythropoietin (EPO) is capable of preventing a wide range of the damage caused by exposure to several chemotherapeutic agents. The results of this work have been so compelling that completing this work was our central focus in the past year, as we now have the first demonstration that it is even possible to identify a single protective agent that can protect multiple cell types and works against multiple chemotherapeutic agents. Moreover, this is a protective agent about which a great deal is known, making this a particularly exciting approach for continued development.

5-FU induced damage to the CNS can be prevented by co-treatment with erythropoietin (EPO)

The fastest path to achieving neuroprotection in the clinic would be to find new uses of existing treatments. The first compound we have examined in this regard is EPO, which is widely used to treat chemotherapy-induced anemia and also shows promise as a neuroprotective agent in experimental studies on traumatic CNS injury [1-12]. Moreover, a recent small pilot study suggests EPO may improve cognitive outcomes in breast cancer patients [13].

The results of our initial studies on EPO were very promising: treatment of animals with EPO (2500 U/kg) during or after 5-FU treatment prevented the reductions in numbers of Olig2+ cells (i.e, oligodendrocytes and their progenitors) seen in the corpus callosum (CC) of treated animals at 8 weeks post-treatment. Moreover, treatment with 5-FU prevented long-term 5-FU-induced reductions in cell division in the subventricular zone (SVZ). Ongoing research has demonstrated rescue of myelin at the ultrastructural level and also rescue of nerve conduction velocity in the auditory nerve. Moreover, we have found that EPO can also protect against at least some of the toxic effects of several other chemotherapeutic agents.

EPO protects against 5-FU induced acute and long-term decreases in CNS cell proliferation, but not against acute increases in apoptosis caused by 5-FU exposure

We previously found that one of the most notable side effects of systemic treatment of 5-FU is a prolonged inhibition of cell proliferation in the SVZ, CC and the dentate gyrus (DG) of the hippocampus, with incorporation of 5-bromodeoxyuridine (BrdU) occurring at reduced levels up to six months after just three intraperitoneal injections of 5-FU. Such inhibition may lead to reductions in the pool(s) of stem and progenitor cells that are thought to be important for maintaining normal homeostasis of the brain tissue and repair from injury.

As our previous studies [14] indicate that the most prominent acute effects of 5-FU occur at Day 1 after the completion of treatment, and delayed effects were pronounced at Day 56, we focused our studies on these time points. At both the early (Day 1) and the late (Day 56) time

points, EPO treatment alone did not affect the cell proliferation in all three regions of interest, as indicated by the similar levels of BrdU incorporation as the control groups.

The ability of EPO to protect the dividing cells of the CNS was seen on both days 1 and 56. As shown in [14], at Day 1 after treatment, the 5-FU treated animals showed a significant decrease in the number of BrdU positive cells in the SVZ (77.9±2.9% versus 100±14.4% in control group; $p<0.05$), while the group treated with the combination of EPO and 5-FU showed similar levels of BrdU incorporation in the SVZ (93.7±4.42%) as the control group. A similar result was seen in the SVZ at the Day 56 time point [14], where animals co-treated with EPO showed near-normal percentages of cells incorporating BrdU.

In our present studies, we did not see a reduction in BrdU incorporation in cells of the CC on Day 1, but did see a statistically significant decrease (to 63.5±30% of control levels), at Day 56.

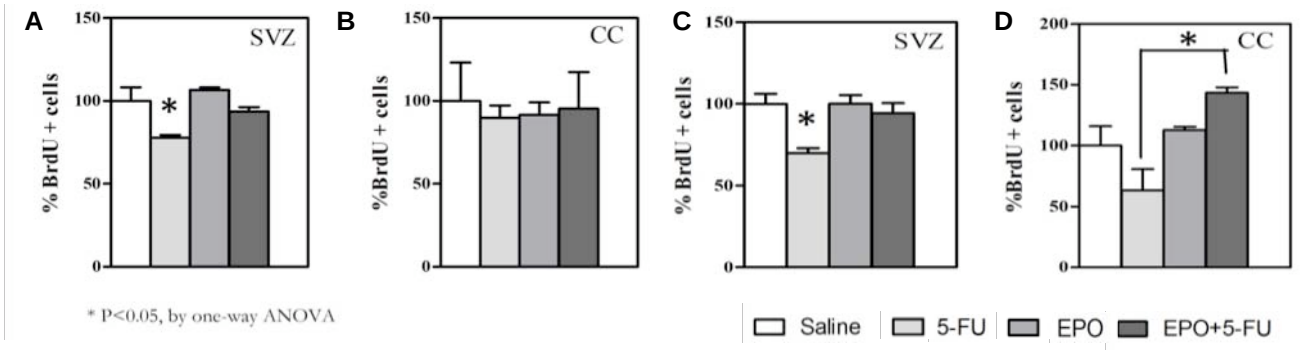

Figure 1. EPO administration prevents the fall in BrdU incorporation caused by 5-FU adminstration. A and B) Sections were analyzed one day after completion of treatment. EPO administration prevented the fall in BrdU incorporation caused by 5-FU exposure. C and D) The fall in BrdU incorporation seen 56 days after completion of 5-FU treatment also is prevented by EPO administration at the time of 5-FU administration.

In contrast, animals treated with 5-FU + EPO showed a higher level of BrdU incorporation even than the control animals, with the combination treated group showing >40% increase in BrdU incorporation over controls (controls = (100±27.8%); EPO only = (113.0±4.6%); EPO + 5-FU = (143.4±7.7%). In the DG, there were no significant differences between any of the 4 groups (data not shown).

Our previous studies showed that one of the acute side effects of systemic 5-FU treatment is a short-term increase short-term increases of apoptosis in the subventricular zone (SVZ), corpus callosum (CC) and dentate gyrus (DG) [14]. In the current study we found that co-treatment of EPO had little effect on this aspect of 5-FU toxicity. For example, as shown in [14] at Day 1, 5-FU caused an over 13-fold increase of TUNEL positive staining in the SVZ, while EPO and 5-FU co-treatment group also had an over 11-fold increase of TUNEL positive staining in the same region compared with the basal level of TUNEL staining in the control group. In the CC, variations between animals was associated with an absence of statistical significance. In the DG, 5-FU induced an over 6-fold increase of TUNEL signals, co-treatment of EPO appeared to bring the TUNEL levels down to near control level, but due to large individual differences among the animals in this treatment group, the effect was not considered statistically significant.

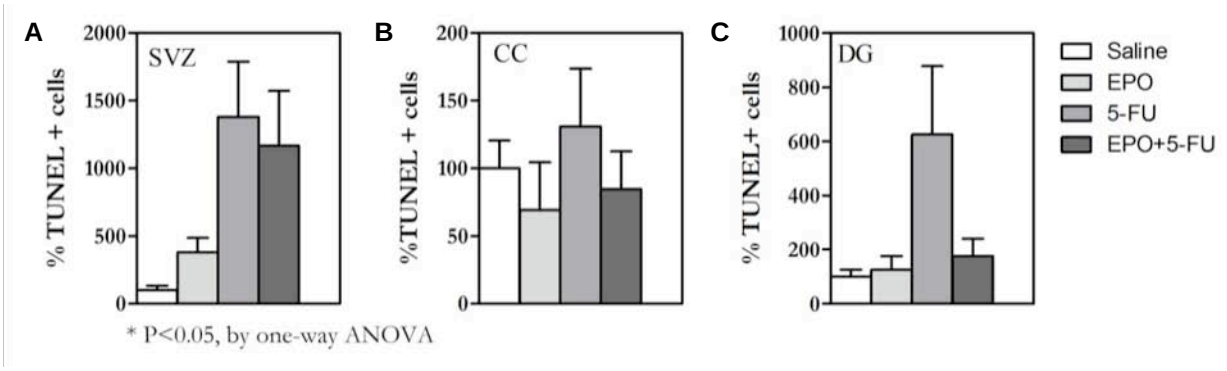

Figure 2. Effects of EPO administration on cell death (as detected by TUNEL labeling) caused by 5-FU administration. Sections were analyzed one day after completion of treatment. In the SVZ and DG there was an increase in TUNEL labeling, although this was not statistically significant due to the range of change that occurred. Nonetheless, the degree of change in the DG was close to achieving statistical significance.

EPO is protective against the long-term myelin and axonal damage caused by 5-FU

In our previous studies we found that 5-FU treatment causes extensive damage of myelin and axons in the corpus callosum at Day 56 after treatment. In the present study, we analyzed electron micrographs of axonal cross sections from the midpoint of the corpus callosum in a quantitative manner to determine whether EPO co-treatment could protect the animals from such damage. Visual examination indicated that 5-FU treated animals showed many patches of abnormally shaped axons, where many axons of larger diameters appeared collapsed and convoluted, and the myelin sheath appeared somewhat thinner. Such pathological patches were mostly absent in other three treatment groups (representative images are shown in (Figure 3A-D). To quantify these changes, we chose 5 randomly selected fields from the cross-section electron micrographs of axon fibers at the mid-point of the corpus callosum to represent each animal, 3 animals per treatment group were imaged, and the NIH Image J program was used to

Comparison of all 4 groups

variable	myelin thickness	diameter	G-ratio	diameter	circularity
p-value	0.025	0.84	0.018	0.81	0.01

Comparison of control, EPO, and 5FU+EPO

variable	myelin thickness	diameter	G-ratio	diameter	circularity
p-value	0.99	0.98	0.99	0.89	0.96

Comparison of control vs. 5FU vs. EPO/control/EPO+5FU

variable	myelin thickness	diameter	G-ratio	diameter	circularity
p-value	0.01	0.71	0.005	0.93	0.005

Table 1. EPO administration prevents the delayed changes in myelin integrity caused by systemic exposure to 5-FU. Electron micrographs of the corpus callosum of animals in each treatment group were analyzed to yield information on myelin thickness, G ratio, axonal circularity. Exposure to 5-FU caused changes in all these paramaters, while co-exposure to EPO prevented such changes.

quantify various parameters of myelin sheaths and axons from each image, such as axonal circularity, axonal diameter, fiber diameter (total diameter of axon including its myelin sheath), and G-ratio (axonal diameter divided by fiber diameter). An average of about 1500 axons from each animal were analyzed, and the distribution of each parameter compiled from 3 animals in each group were compared using a Kolmogorov-Smirnov statistic. Two separate sets of images captured at different magnification were used for the analysis of axonal shape descriptors and myelin parameters. As shown in Figure 3 E-I and Table 1, myelin thickness, G-ratio, and circularity differ among all 4 treatment groups ($p < 0.018$), but no significant difference was found between axonal diameters ($p > 0.84$).

Our studies demonstrated that EPO treatment conferred protection against the effects of 5FU on myelin integrity. 5FU treatment caused significant alterations in myelin thickness, G-ratio, and circularity ($p < 0.01$), but not diameter ($p > 0.71$). In contrast, when looking at all 4 of these variables among the control, EPO, and EPO+5FU groups, no differences could be detected ($p > 0.89$). In other words, EPO administration prevented the delayed damage to myelin integrity caused by 5FU exposure.

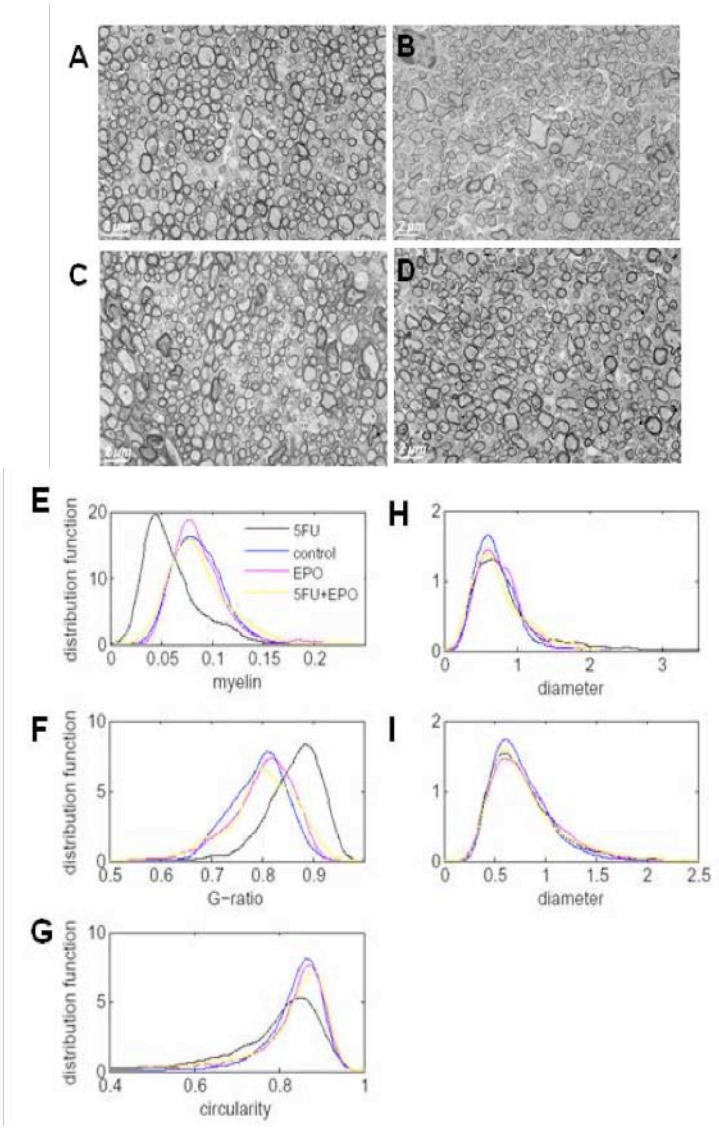

Figure 3. EPO administration prevents the delayed changes in myelin integrity caused by systemic 5-FU exposure. A-D) Representative sections from animals treated with vehicle (A), 5-FU (B), EPO (C) or 5-FU + EPO (D). E-H shows the distribution of values for the various parameters analyzed in these studies. As shown, 5-FU treated animals showed differences in myelin thickness (E), G-ratio (F) and circularity (G). In contrast, axonal diameter (H) and fiber diameter (total diameter of axon including its myelin sheath) were unchanged. An average of about 1500 axons from each animal were analyzed, and the distribution of each parameter compiled from 3 animals in each group were compared using Kolmogorov-Smirnov statistics.

These results are consistent with our previous finding that 5-FU treatment caused diffuse myelin and axonal damage at this late time point [14], while animals that received EPO co-treatment appears to be normal in these regards. With 5-FU treatment there were patches of pathologic changes of thinning myelin sheaths and increased G-ratio. The G-ratio is one of the parameters used widely to describe myelin pathology. It is generally thought that G-ratio is tightly controlled to maximize nervous conductivity. Increased G-ratio is frequently associated with decreased nerve conduction velocity. In the CC the normal range of G-ratio in mice is between 0.75-0.81. Because the axon caliber is unchanged by the treatment, the increase in G-ratio appears mainly caused by the decrease in myelin thickness in 5-FU group. Taken together, these results indicate that 5-FU treatment resulted in decreases of myelin thickness, increases in G ratio and decreases in axonal circularity, all of which have been indicated to cause decrease in conduction velocity; while co-administration of EPO protects against these changes. Also, in spite of extensive myelin and axonal abnormality caused by 5-FU treatment, there was no loss of axons at this time point, nor did EPO or the combinatorial treatment cause any changes in this regard (data not shown).

5-FU treatment caused delayed onset and persistent elongation of auditory brainstem response inter-peak latencies, which is prevented by co-treatment of EPO

It is of critical importance to bring together cellular and functional analysis, and even more so to develop functional analyses that have the potential of being utilized in patient populations. To this end, we have been using analysis of conduction velocity in the auditory nerve (also known as the auditory brainstem response, or ABR) in order to obtain information about the functional status of myelination. As loss of myelin integrity causes decreases in conduction velocity (i.e, increases in the latency of signal propagation), changes in the speed of impulse conduction can be used as a functional indicator of this type of damage.

Having found myelin damage at the ultrastructural level in animals exposed to 5-FU, and having found that EPO co-treatment protected the myelin and axons against the damages caused by

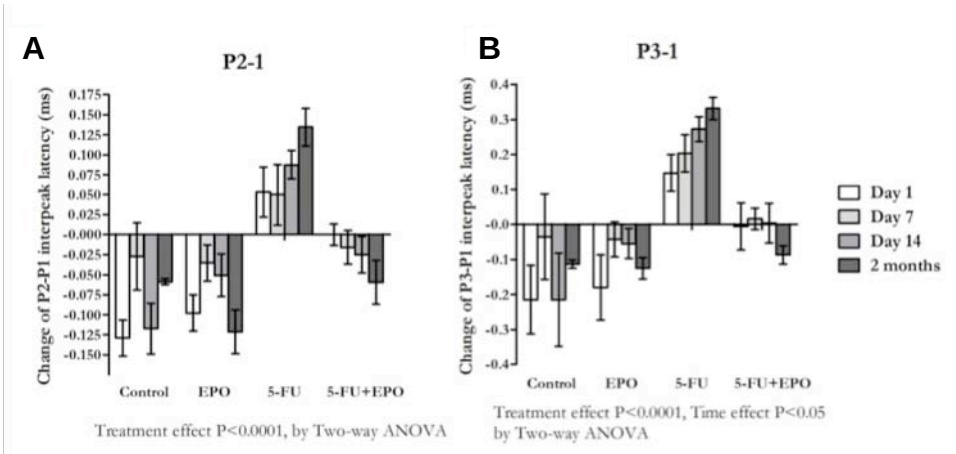

Figure 4. EPO administration prevents the changes in ABR latency caused by 5-FU exposure. We analyzed ABR peaks and calculated P2-1 and P3-1 latencies in all four treatment groups. As shown, animals treated with 5-FU showed marked decreases in the speed of impulse conduction, as predicted by the degradation of myelin integrity shown in Table 1 and Figure 3. These changes were largely prevented in animals also exposed to EPO.

this agent, we next examined the ABR response in each of our 4 treatment groups. Auditory function tests were conducted as described previously [14] to examine whether there is corresponding functional protection in live animals. For hearing tests, a dedicated set of mice were first tested for their baseline hearing functions before they received any treatment, and the baseline measurements of auditory function parameters of each individual animal were used later to compute changes after treatment at various time points to reduce data variability caused by individual difference. The mice were treated with saline, EPO, 5-FU or EPO+5-FU as described earlier, and tested for hearing at Day1, Day 14 and Day 56 time points. In these studies, we examined the distortion product otoacoustic emissions (DPOAE) as an indicator of cochlear function and the auditory brainstem responses (ABR) to provide information on changes in conduction velocity from the ear to the brain, an indicator of myelination status. Different peaks in the ABR response waveforms are thought to correspond to different stages in the transmission of auditory information, and prior analysis of ABR inter-peak latencies shows that loss of myelin causes increases in specific ABR inter-peak latencies (P2-P1 and P3-P1). Such measurements have been used by multiple investigators to study myelination-associated problems in impulse conduction in children with iron deficiency. Our previous study revealed that 5-FU treatment was associated with increased inter-peak latencies of ABR at delayed time points, and that 5-FU did not cause any changes in cochlear function as indicated by DPOAE test results.

Our studies on EPO-mediated protection demonstrated that concurrent administration of EPO with 5-FU prevents the adverse effects of 5-FU had on ABR latencies. As shown in Figure 4, at 11.3kHz 70dB sound stimulus, the 5-FU treated group had significant increases at both inter-peak latencies P2-1 and P3-1, while all other 3 treatment groups had no change or decreases in the inter-peak latency values. Consistent with previous studies, 5-FU did not cause changes in the DPOAE test, nor did EPO or the combinatorial treatment . These results indicate that the changes we saw in ABR tests do not involve hair cell injury, but are more directly related to the myelination deficits that were evident in our electron microscopy studies of the CNS white matter. Loss of myelin, increases in G-ratio and decreases in axon circularity all have the potential of causing alterations in nervous conduction velocity and elongation of ABR inter-peak latencies. Similar results were seen at several other frequencies tested ranging from 5.6 kHz to 32 kHz (data not shown).

5-FU treatment did not seem to cause as much damage in the peripheral nervous compartment of the auditory system, since there was no significant change in Peak 1 latency at all time points examined (data not shown).

EPO exposure prevents multiple adverse effects of systemic cisplatin exposure on the CNS

We next examined the ability of EPO to protect against damage caused by cisplatin, an alkylating chemotherapeutic agent with a very different mechanism that 5-FU (which is an anti-metabolite). We previously found that systemic exposure to cisplatin is also associated with damage to the CNS, causing increases in cell death and decreases in cell division in the SVZ, CC and DG. We re-examined these parameters in animals treated with cisplatin with or without co-exposure to EPO.

EPO exposure also was able to prevent cisplatin-induced decreases in neuronal progenitor cells in the adult hippocampus. One day after the completion of cisplatin treatment, we saw decreases in both proliferating (Ki67+) and non-proliferating (Ki67-) neuroblasts (identified by

doublecortin (DCX) expression. EPO co-administration prevented cisplatin induced changes to both of these populations.

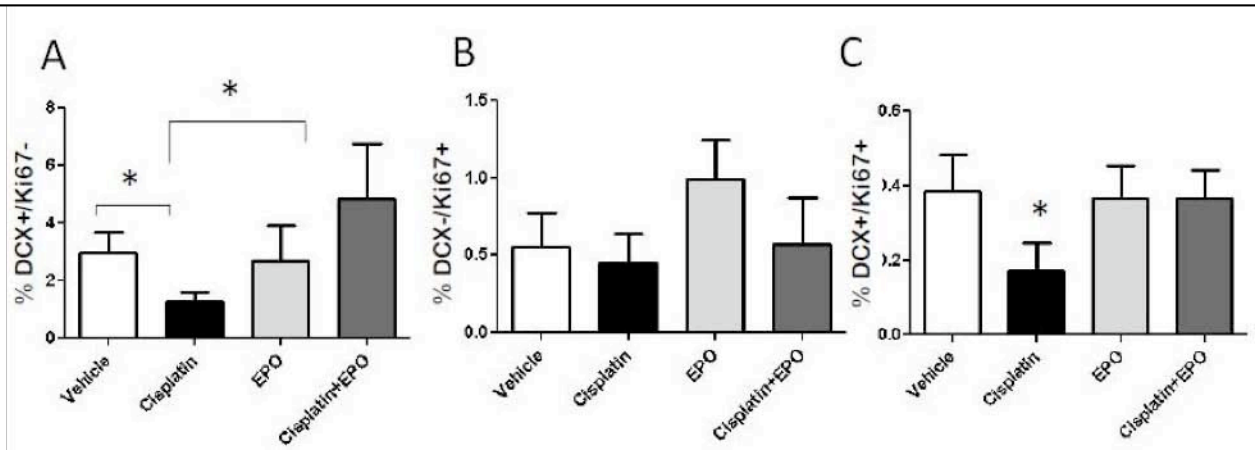

Figure 5. EPO exposure also was able to prevent cisplatin-induced decreases in neuronal progenitor cells in the adult hippocampus. One day after the completion of cisplatin treatment, we saw decreases in both proliferating (Ki67+) and non-proliferating (Ki67-) neuroblasts (identified by doublecortin (DCX) expression. EPO co-administration prevented cisplatin induced changes to both non-dividing populations (A) and dividing populations (B and C).

We also found that EPO protected oligodendrocytes of the CC from the effects of cisplatin, but did not protect dividing glial progenitor cells. Staining with anti-Olig2 antibody was combined with Ki67 staining to distinguish oligodendrocytes (Olig2+/Ki67-) from proliferating oligodendrocyte progenitor cells (Olig2+/Ki67+). Cisplatin exposure caused a significant decrease in the proportionate representation of oligodendrocytes

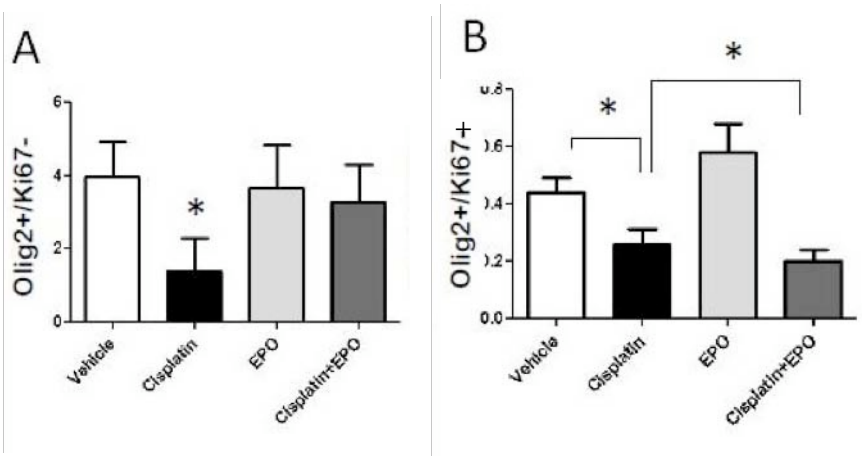

Figure 6. EPO protected oligodendrocytes of the CC from the effects of cisplatin, but did not protect dividing glial progenitor cells. Staining with anti-Olig2 antibody was combined with Ki67 staining to distinguish oligodendrocytes (Olig2+/Ki67-) from proliferating oligodendrocyte progenitor cells (Olig2+/Ki67+). (A) Cisplatin exposure caused a significant decrease in the proportionate representation of oligodendrocytes among total DAPI+ cells in the CC, and this decrease was prevented by co-exposure to EPO. In contrast, although cisplatin exposure also caused a significant reduction in the representation of oligodendrocyte progenitor cells, EPO co-exposure did not rescue this population.

among total DAPI+ cells in the CC, and this decrease was prevented by co-exposure to EPO. In contrast, although cisplatin exposure also caused a significant reduction in the representation of oligodendrocyte progenitor cells, EPO co-exposure did not rescue this population.

As children are also susceptible to toxic effects of chemotherapy on the CNS, we next exposed younger animals to two agents frequently used in the treatment of pediatric disease, vincristine (an anti-mitotic agent that prevents normal microtubule assembly and which is used in the treatment of lympohomas, acute lympoblastic leukemia and nephroblastoma) and cyclophosphamide (an aklylating agent of lymphomas, leukemia and some solid tumors). In these studies, 3 week old mice were treated with (*details), in the presence or absence of EPO, and examined one day after the completion of treatment for effects on cell division and cell death. As we have not previously examined the effects of these drugs, nor have we examined such young animals, we also stained tissues with antibodies chosen to reveal additional information about affected cell types.

The SVZ of mice treated with vincristine showed a significant decrease in dividing cells and this decrease was prevented by co-administration of EPO. Mice exposed to vincristine showed a >60% decrease in the representation of dividing cells that did not express PSA-NCAM (a marker of migratory progenitor cells), In contrast, animals co-exposed to EPO showed no such decrease. In distinction from the effects on PSA-NCAM-negative cells, there was no effect of vincristine treatment on the PSA-NCAM expressing cells of the SVZ.

Analysis of cell division in the DG also revealed a protective effect of EPO, this time on non-dividing neuronal progenitor cells (identified as DCX+/Ki67- cells) that was prevented by EPO treatment. There was a >60% decrease in the representation of these cells among the total DAPI+ population of the DG. In contrast, in animals treated with EPO there was a significant increase in the representation of these cells among the total cells of the DG. Dividing neuronal progenitor cells (PSA-NCAM+/Ki67+) were not significantly reduced in these animals, but animals treated with EPO and vincristine showed a significant increase.

Cyclophosphamide exposure also caused a reduction in the representation of dividing neuronal progenitor cells in the SVZ, but EPO had no protective effect on these cells. Nor did EPO exposure protect against the reductions in PSA-NCAM+ cells that were Ki67-. In contrast, EPO did prevent cyclophosphamide-induced cell death in the SVZ. Exposure to cyclophosphamide caused a >3-fold increase in TUNEL staining in PSA-NCAM+ cells, a change that was almost entirely prevented by co-administration of EPO. Among the PSA-NCAM- cells, there was a > 9-fold increase in the representation of TUNEL+ cells. Co-exposure to EPO reduced this to an ~6-fold increase, which was not significantly different from the level of cell death in either vehicle- or vincristine-treated cells.

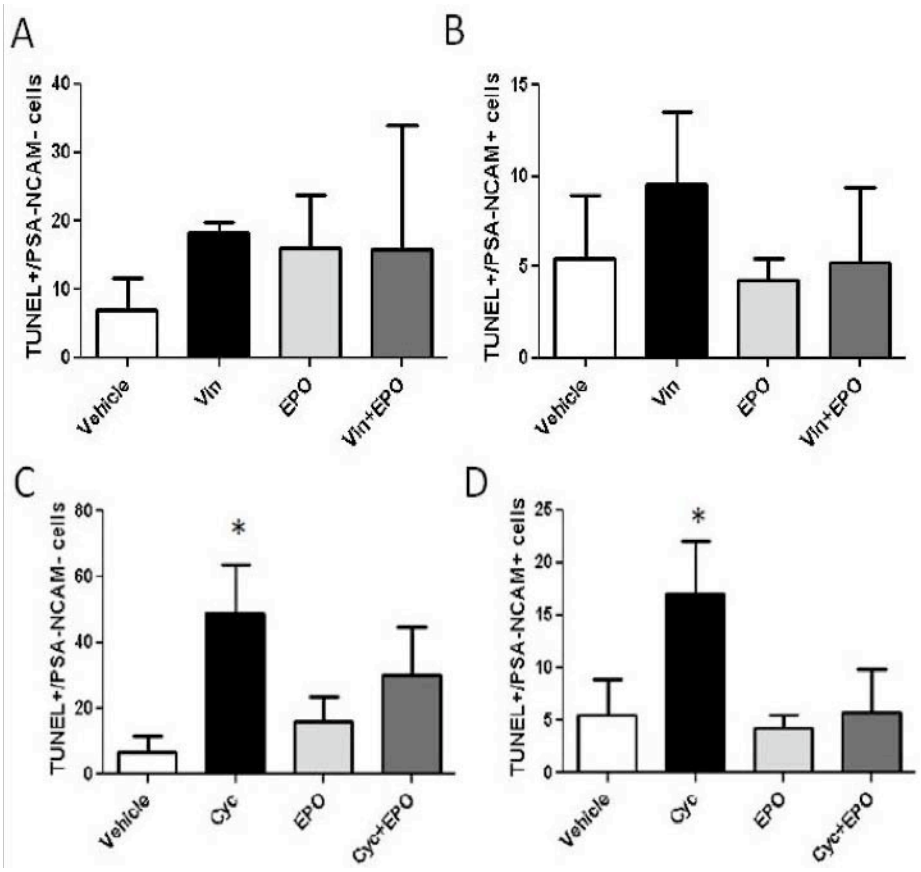

Figure 7. EPO prevented cyclophosphamide-induced cell death in the SVZ. Co-exposure to EPO reduced this to an ~6-fold increase, which was not significantly different from the level of cell death in either vehicle- or vincristine-treated cells (C). Exposure to cyclophosphamide caused a >3-fold increase in TUNEL staining in PSA-NCAM+ cells, a change that was almost entirely prevented by co-administration of EPO (D).

Key Research Accomplishments

We have discovered a remarkable protective capacity of EPO against neurotoxic activities of 5-FU, cisplatin, cyclophosphamide and vincristine. These studies have defined multiple parameters relevant to the study of these toxicity reactions and provide the first demonsration that a single biological agent can provide wide-ranging protection.

Reportable outcomes

Pending

Conclusions

EPO represents the first example of a protective agent that is capable of preventing mujltiple toxicities of a variety of chemotherapeutic agents. By demonstrating that such protection is possible, this work should now open the door to much more widespread entry into this important new arena of cancer research.

References

1. Kellert, B.A., R.J. McPherson, and S.E. Juul, *A comparison of high-dose recombinant erythropoietin treatment regimens in brain-injured neonatal rats.* Pediatr Res, 2007. 61(4): p. 451-5.

2. Keogh, C.L., S.P. Yu, and L. Wei, *The effect of recombinant human EPO on neurovasculature repair after focal ischemic stroke in neonatal rats.* J. Pharmacol. Exp. Ther., 2007.
3. Won, Y.J., et al., *Erythropoietin is neuroprotective on GABAergic neurons against kainic acid-excitotoxicity in the rat spinal cell cultures.* Brain Res, 2007.
4. Cherian, L., C.J. Goodman, and C.S. Robertson, *Neuroprotection with Erythropoietin Administration Following Controlled Cortical Impact Injury in Rats.* J Pharmacol Exp Ther, 2007.
5. Koh, S.H., et al., *Recombinant human erythropoietin suppresses symptom onset and progression of G93A-SOD1 mouse model of ALS by preventing motor neuron death and inflammation.* Eur J Neurosci, 2007. 25(7): p. 1923-30.
6. Sonmez, A., et al., *Erythropoietin attenuates neuronal injury and potentiates the expression of pCREB in anterior horn after transient spinal cord ischemia in rats.* Surg Neurol, 2007.
7. Xue, Y.Q., et al., *Intrastriatal administration of erythropoietin protects dopaminergic neurons and improves neurobehavioral outcome in a rat model of Parkinson's disease.* Neuroscience, 2007. 146(3): p. 1245-58.
8. Tonges, L., et al., *Hematopoietic cytokines--on the verge of conquering neurology.* Curr Mol Med, 2007. 7(2): p. 157-70.
9. Zhong, L., et al., *Erythropoietin promotes survival of retinal ganglion cells in DBA/2J glaucoma mice.* Invest Ophthalmol Vis Sci, 2007. 48(3): p. 1212-8.
10. Bianchi, R., et al., *Cisplatin-induced peripheral neuropathy: neuroprotection by erythropoietin without affecting tumour growth.* Eur J Cancer, 2007. 43(4): p. 710-7.
11. Nadam, J., et al., *Neuroprotective effects of erythropoietin in the rat hippocampus after pilocarpine-induced status epilepticus.* Neurobiol Dis, 2007. 25(2): p. 412-26.
12. Vitellaro-Zuccarello, L., et al., *Erythropoietin-mediated preservation of the white matter in rat spinal cord injury.* Neuroscience, 2007. 144(3): p. 865-77.
13. O'Shaughnessy, J.A., et al., *Feasibility of quantifying the effects of epoetin alfa therapy on cognitive function in women with breast cancer undergoing adjuvant or neoadjuvant chemotherapy.* Clin. Breast Cancer, 2005. 5: p. 439-446.
14. Han, R., et al., *Systemic 5-fluorouracil treatment causes a syndrome of delayed myelin destruction in the CNS.* J. Biol., 2008. 7( ): p. e12.

Appendices
N/A

Melampomagnolide B, a new antileukemic sesquiterpene

Leave this area blank for abstract info.

Shama Nasim[1], ShanShan Pei[2*], Fred K. Hagen[3], Craig T. Jordan[2,4], Peter A. Crooks[1**]*

[1]Department of Pharmaceutical Sciences, College of Pharmacy, University of Kentucky, Lexington, KY 40536, USA[2]Department of Biomedical Genetics, [3]Rochester Proteomics Center, Department of Biochemistry and Biophysics, [4]James P. Wilmot Cancer Center, University of Rochester, Rochester, NY 14642, USA

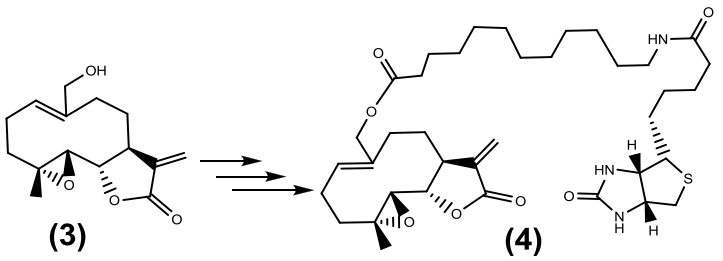

Melampomagnolide B (**3**) has been identified as a new antileukemic sesquiterpene. A biotin-conjugated derivative (**4**) of melampomagnolide B was designed and synthesized in order to elucidate its mechanism of action. A study of the biochemical interactions of the biotin probe suggests that melampomagnolide B derives its remarkable selectivity for leukemic cells over normal hematopoietic cells from its unique ability to exploit biochemical differences between the two cell types.

Graphical Abstract

Pergamon

BIOORGANIC & MEDICINAL CHEMISTRY

Melampomagnolide B: a new antileukemic sesquiterpene

Shama Nasim[1*], ShanShan Pei[2*], Fred K. Hagen[3], Craig T. Jordan[2,4], Peter A Crooks[1**]

[1]Department of Pharmaceutical Sciences, College of Pharmacy, University of Kentucky, Lexington, KY 40536, USA

[2]Department of Biomedical Genetics, [3]Rochester Proteomics Center, Department of Biochemistry and Biophysics, [4]James P. Wilmot Cancer Center, University of Rochester, Rochester, NY 14642, USA

Abstract— Melampomagnolide B has been identified as a new antileukemic sesequiterpene. A biotin-conjugated derivative of melampomagnolide B was designed and synthesized in order to elucidate its mechanism of action. A study of the biochemical interactions of the biotin probe suggests that malampomagnolide B derives its remarkable selectivity for leukemic cells over normal hematopoietic cells from its unique ability to exploit biochemical differences between the two cell types.

1. Introduction

The past several years have seen a surge of interest in the anticancer properties of sesquiterpene lactones. A germacrenolide, parthenolide (PTL, **1**, Figure 1) has been noted for its remarkable antileukemic properties.[1] Initial efforts pertaining to the biomechanistic study of parthenolide and its analogs revealed that they seem to promote apoptosis by inhibiting the activity of the NF-κB transcription factor complex, and thereby down-regulating anti-apoptotic genes under NF-κB control.[2-7] We have recently demonstrated that parthenolide induces robust apoptosis of primary acute myeloid leukemic (AML) cells.[8,9] In particular, parthenolide causes cell death in AML stem and progenitor cells in vitro, with minimal toxicity towards normal hematopoietic cells. The apoptosis induced by parthenolide is not solely due to NF-κB inhibition, but rather arises from a broad set of biological responses, which likely include activation of p53 and an increase in reactive oxygen species. Parthenolide has also been the source of several novel antileukemic compounds arising from our program over the past decade. We successfully overcame the poor water-solubility of parthenolide by adding amines to the exocyclic olefin of the enone function of **1**, thereby rendering the resulting compounds water-soluble.[10,11] Such adducts showed retention of antileukemic properties of parthenolide; in particular, the dimethylamine-adduct of parthenolide (DMAPT, LC-1, **2**, Figure 1), which has progressed to phase-I clinical trials in the United Kingdom for the treatment of AML, ALL and CLL.[10]

We now report on the identification of melampomagnolide B (MMB, **3**, Figure 1), a melampolide originally isolated from *Magnolia grandiflora*,[12] as a new antileukemic sesquiterpene with properties similar to parthenolide. MMB was synthesized utilizing a modification of the method of Macias et al.[13] via selenium oxide oxidation of the C10 methyl group of PTL, which also results in concomitant conversion of the geometry of the C9-C10 double bond from *trans* to *cis*. This compound is of great interest to us for two reasons. First, the anti-leukemia activity of MMB is excellent, and indistinguishable from PTL. Second, as a functionalized analog of PTL, the MMB molecule allows the synthesis of conjugated analogs that retain biological activity. For example, as a laboratory tool, we created a biotinylated analog of MMB via conjugation at the allylic hydroxyl group, and used this reagent to identify MMB target proteins in AML cells. This approach has proven to be extremely useful in better understanding the underlying mechanisms by which anti-leukemia activity is achieved. Thus, as a basis for the further development of this drug, we sought to perform comprehensive analysis of drug mechanism. To this end, we initiated a program that focused on delineating the cellular proteins and signaling cascades influenced by **3** or its analogs. One branch of this program is to synthesize chemical probes based on **3** that would retain its antileukemic potential, but contain a "reporter" or a marker that could serve to highlight the subcellular localization or biochemical interactions of the probe. This report describes the first of such efforts, which sought to utilize the potential of a biotin moiety in highlighting the interactions of **3** with cellular proteins, as well as to study its localization into organelles through microscopy. In the present study, we describe the chemical synthesis of a biotinylated analog of **3** and demonstrate that this compound is a robust agent for the identification of protein binding events.

*These authors contributed equally to this work

**Corresponding author. Tel.: +1 859-257-1718; fax: +1 859-257-7585. E-mail: pcrooks@email.uky.edu (P.A.Crooks).

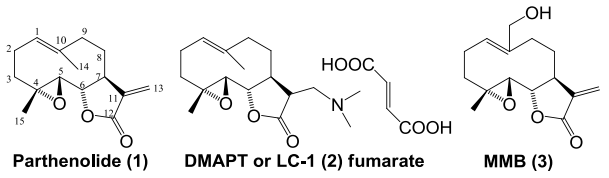

Figure 1. Structures of PTL (**1**), DMAPT (**2**) and MMB **(3)**

2. Design Rationale and Antileukemic Activity Studies

A biotin analog of **3** that involved the conjugation of the allylic hydroxyl group with a suitable biotinylated moiety to afford **4** was synthesized. The utilization of this probe presented an opportunity to identify all proteins directly modified by **3**, and thereby reveal other mechanisms contributing to anti-leukemic activity of MMB.

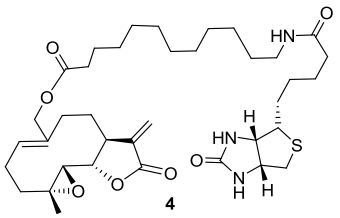

Figure 2. Structure of the biotinylated MMB probe (**4)**

3. Chemistry

The synthesis of **4** utilized PTL as starting material, via selenium oxide oxidation of the allylic methyl group applying a modification of the method of Macias et al.[13] The allylic methyl group of PTL was subjected to SeO_2/t-BuOOH oxidation, yielding a mixture of MMB (**3**) and aldehyde **5**. This reaction proved to be particularly fickle, with the aldehyde **5** being the major side-product that formed in significant quantities and impaired chromatographic isolation of **3**. There was a significant variation in the quantitiy of **5** formed in relation to **3**. For optimal oxidation of **1** to MMB (**3**), the literature procedure prescribes a combination of SeO_2 and *t*-Butyl hydroperoxide, which in our hands afforded a mixture of the required alcohol **3** and the aldehyde **5** in approximately a 1:1 ratio. While the quality of *t*-butyl hydroperoxide was inconsequential to the ratio, the quality (purity) of SeO_2 was found to be very important. Samples that possessed the characteristic pink color of selenium were found to afford higher quantities of **5**, at the expense of **3**. In addition, alcohol **3** could only be separated from **5** with difficulty by silica gel chromatography. NMR spectroscopic analysis was consistent with the structural assignments reported by Macias et al.[13], and an x-ray crystal structure obtained in our hands was identical to that previously reported by Gonzalez et al.[14] A Mitsunobu reaction on **3** with Fmoc-protected 12-aminododecanoic acid afforded **6**. While the use of morpholine/piperidine is common for Fmoc deprotections, this transformation had to be carried out with TBAF instead, due to the possibility of morpholine/piperidine adding to the enone function of **6**. The amine **7**, formed *in-situ*, was treated directly with the pentafluorophenyl ester of biotin to afford the target compound **4**. Purification of this reaction mixture proved to be challenging, with the best conditions being the elution of the evaporated reaction mixture from an Et_3N-treated silica column with a gradient of *i*-PrOH in CH_2Cl_2. It should also be noted that the germacrenolide ring of **3** seemed to be susceptible to the basicitiy of F^- from TBAF, with numerous by-products being formed that lacked the Fmoc-dodecanoic acid-biotin appendage, according to NMR spectral data. The identity of these by-products was not

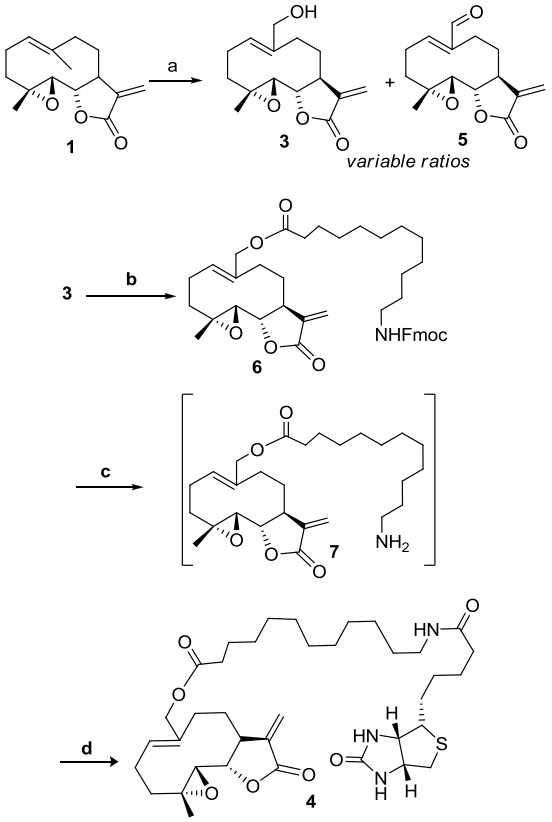

a: SeO_2, tert.BuOOH, CH_2Cl_2, 1.5 h, 40 ^oC, 50 %; b: Fmoc-protected dodecanoic acid, Ph_3P, DIEAD, rt, 18 h, 68 %; c: TBAF, DMF, 30 min, d: Biotin pentaflurophenol, 18 h, rt, 45 %.

Scheme 1. Synthesis of **3** from **1**, and conjugation of biotin to **3.**

determined. The use of other coupling reagents, i.e. HATU and EDC, afforded reaction mixtures that could not be resolved on silica so as to afford **4** in an analytically pure form.

4. Antileukemic Properties of 4

To validate the retention of functional properties, the activity of **3** and **4** were compared to **1** using assays that measure inhibition of NF-κB activity. Primary leukemia cells were treated with varying concentrations of **1**, **3** or **4** for six hours, followed by lysis and analysis by immunoblot. Inhibition of NF-κB activity was assessed by measuring phosphorylation of the NF-κB p65 subunit at Ser-536. As shown in Figure 3A, a significant loss of phosphorylation is observed for **3** at 7.5 μM concentration, and for **4** at 20 μM concentration. To further evaluate the cytoxicity of **3** and **4**, cell viability was measured following 24 h exposure to each compound. As shown in Figure 3B, efficient induction of cell death is achieved at 7.5 μM **3**. To achieve a similar degree of cell death with **4**, treatment at 20-30 μM was required, in good agreement with the NF-κB phosphorylation analysis shown in Figure 3A. Thus, while **3** and **4** retain the biological properties of **1**, the

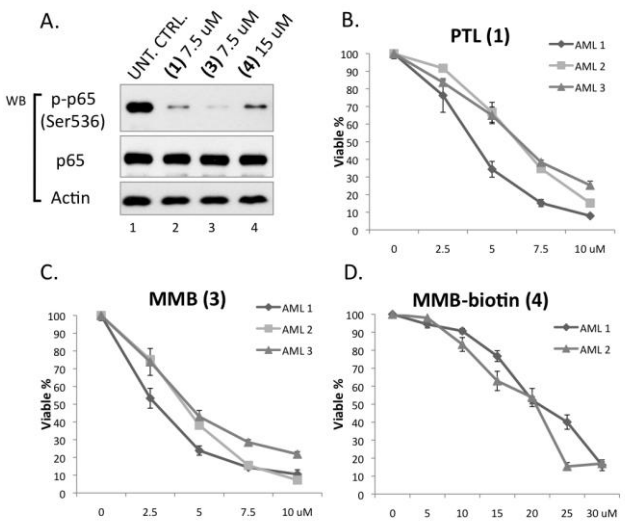

Figure 3. Biological activities of **4** compared to **1** and **3**. A) Immunoblot of phosphorylated p65 subunit of the NF-kB complex. Also shown are total p65 and actin. B-D) Viability of primary leukemia cells after overnight culture at varying concentrations.

activity of **4** is reduced approximately 2-fold. We attribute this minor loss in activity to steric hindrance resulting from the addition of the bulky biotin moiety. We compared the activities of **1** and **3**. Allylic alcohol **3** was found to possess potency and selectivity similar to **1**. Thus, MMB is active in spite of being a melampolide and not a germacrenolide, and further studies into the newly found antileukemic activity of **3** are warranted.

Subsequent studies employed **4** as a reagent to identify potential leukemic proteins modified by MMB. Primary human cells were treated with 20 μM **4** for 6 h, followed by lysis and immunoblot analysis using a streptavidin probe. As shown in Figure 4, multiple protein targets were identified in the whole cell lysates. Notably, the analysis of normal bone marrow (NBM) cells (lane 2) in comparison to acute myeloid leukemia (AML) cells (lane 3) indicates distinct differences in the spectrum of cellular targets, even though the identical protein–compound **4** ratio is used for normal and leukemic preparations (*marks a non-specific band recognized by SA-HRP probe). Thus, while the chemistry of **4** should be essentially the same in any cell type, there must be intrinsic differences between normal and leukemic cells that lead to the interaction with unique targets. We propose that this differential binding contributes to the leukemia-specific cell death previously described for **1**. To further validate the utility of **4** for analysis of protein targets, we performed biochemical pull-down studies. Previous studies have demonstrated that biotinylated **1** binds to the NF-κB regulatory protein IKK-β.[15] Therefore, we tested whether **4** would also bind this

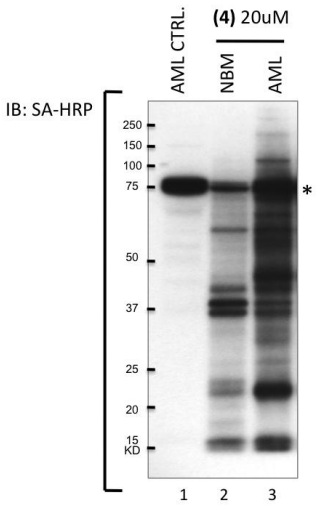

Figure 4. Immunoblot analysis of whole cell protein lysates. Lane 1 shows control using AML protein probed with biotin to detect non-specific interactions. Lanes 2 and 3 are normal bone marrow (NBM) lysate and AML respectively, probed with analog **4**.

protein. In Figure 5, primary leukemia cells were pre-treated for 2 h with **1** (lanes 2, 5) or biotin control (b.c.) (lanes 3,6), prior to a 4 h incubation with **4**. Cells were then lysed and immuno-precipitated by streptavidin beads. Pull-down products were analyzed by immunoblot to identify specific proteins. As shown in Figure 5, one product identified was IKK-β, the known target of **1**[15,16], thereby validating the specificity of the reagent for targets relevant to the anti-leukemia mechanism of action. In addition, the NF-κB p65 subunit was identified as a direct target in the pull-down, suggesting interactions with multiple components of the NF-κB signaling pathway. Notably, pre-incubation with **1** potently reduced binding of IKK-β or

p65 to **4** (lane 5), indicating such binding between IKK-β or p65 and **4** is through the same mechanism between IKK-β or p65 and **1**.

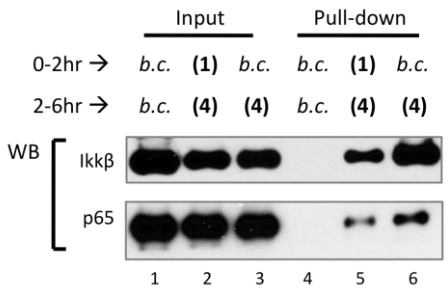

Figure 5. Identification of MMB binding proteins. Analog **4** was used for pull-down studies to identify specific target proteins. As indicated above each lane, specimens were subjected to a 2-hour pre-incubation with either parthenolide (**1**) or a biotin control (*b.c.*) to test specificity of subsequent interactions. Next, each specimen was incubated for 4-hours with either analog **4** or biotin control. Lanes 1-3 show total input lysate for the three independent conditions. Lanes 4-6 show pull-downs for the same conditions shown in lanes 1-3. Input or pull-down products were probed with antibodies to the NF-κB regulator IKK-β or the NF-κB subunit p65. As shown in lane 6, both IKKβ and p65 were successfully detected by pull-down. Lane 5 indicates that pre-incubation with **1** successfully competes for binding with **4**, thereby indicating specificity of the pull-down for **4**.

5. Summary

Taken together, these data show that malampomagnolide B is a new antileukemic agent with remarkable selectivity for leukemic cells over normal hematopoietic cells. This selectivity is derived from its unique ability to exploit biochemical differences between the two cell types. The study also demonstrates the utility of the biotin conjugate **4** for the identification of protein binding targets of both **3** and **1**. Additional studies are ongoing to identify all the proteins that interact with **4**.

6. Experimental

Biotin was purchased from AK Scientific, Inc, Mountain View, CA. All other reagents and chemicals were purchased from Aldrich Chemical Co., Milwaukee, WI. THF and diethyl ether were distilled over sodium-benzophenone ketyl and stored under argon. All other solvents and chemicals were used as received. TLC analyses were run on Analtech Silica Gel GF® plates. Melting points were determined on a Fisher Scientific melting point apparatus and are uncorrected. NMR spectra were run on a Varian 300 MHz NMR spectrometer in $CDCl_3$ and chemical shifts are reported in ppm relative to TMS as internal standard. Mass spectra were recorded on a JEO: JMS-700T MStation or on a Bruker Autoflex MALDI-TOF MS. DMF was either distilled over P_2O_5 immediately before use or the anhydrous grade from Aldrich® was used. Parthenolide was purchased from Aldrich (St.Louis, MO). CHN analysis was performed by Atlantic Micro Labs, and are within ±0.4% of theoretical values. The synthesis of compound **3** has been reported elsewhere[13], and its characterization data are in good agreement with reported values.

6.1 Synthetic procedures for the synthesis of compounds 3, 4 and 6.

6.1.1. Melampomagnolide B (3). A solution of **1** (250.0 mg, 1.0 mmol) in CH_2Cl_2 was treated with SeO_2 (111.0 mg, 1.0 mmol) and *tert*-butyl hydroperoxide (1M in dodecane, 1 mL) and the mixture was refluxed gently for an hour, after which it was evaporated. The resulting semisolid was subjected to silica gel chromatography to afford **3** (132.0 mg, 50%). Hexane/acetone = 85: 15); White crystals; MP 172–176 °C; ^{1}H NMR (300 MHz, $CDCl_3$) δ 6.25 (app. , J = 10.0 Hz, 1H), 5.66 (app. t, J = 6 Hz, 1H), 6.56 (app. d , J = 10.0 Hz, 1H), 4.12 (q, J = 12.6 Hz, 2H), 3.86 (t, J = 9.6 Hz, 1H), 2.83 (m, 2H), 2.49–1.13 (m, 5H), 1.72–092 (m, 2H), 1.56 (s, 3H) ppm. ^{13}C NMR (75 MHz, $CDCl_3$) δ 169.5, 139.6, 138.9, 127.7, 120.3, 81.3, 66.1, 63.6, 60.3, 43.1, 37.1, 25.9, 24.2, 24.0, 18.3 ppm; EI-MS *m/z*; 264.

6.1.2. 14-(*N*-fmoc-12-Aminododecanoxy)melampomagnolide B (6). A solution of **3** (264 mg, 1 mmol), Fmoc-dodecanoic acid (437 mg, 1 mmol) and Ph_3P (262 mg, 1 mmol) in THF (3 mL) was treated drop-wise with diethyl azodicarboxylate until a yellow color persisted. The resulting solution was stirred for 12 h at room temperature and then evaporated to afford a semisolid that was subjected to silica gel chromatography (hexane/acetone, 9: 1) to afford **6** (463.0 mg, 68%) as a colorless oil. ^{1}H NMR (300 MHz, $CDCl_3$) δ 7.73 (d, J = 7.5 Hz, 2H), 7.59 (d, J = 7.5 Hz, 2H), 7.42–7.25 (m, 4H), 6.25 (d, J = 3.6 Hz, 1H), 5.67 (app. t, J = 8.1 Hz, 1H), 5.53 (d , J = 3.0 Hz, 1H), 4.78 (brd. s, 1H), 4.65 (d, J = 12.3 Hz, 1H), 4.46–4.19 (m, 5H), 3.84 (t, J = 9.3 Hz, 1H), 3.19 (m, 2H), 2.93–2.83 (m, 2H), 2.45–2.11 (m, 6H), 1.43–0.87 (m, 21 H), 1.53 (s, 3H) ppm. ^{13}C NMR (75 MHz, $CDCl_3$) δ 173.5, 169.4, 156.5, 144.1, 141.4, 138.8, 135.0, 130.7, 127.7, 127.1, 125.1, 120.4, 120.1, 81.2, 66.77, 66. 71, 63.5, 60.21, 47.5, 42.9, 41.3, 36.9, 34.5, 30.2, 29.8, 29.7, 29.5, 29.4, 27.0, 26.0, 25.2, 24.8, 24.1, 18.3 ppm. ESI-MS *m/z*: 683 $(M+H)^+$.

6.1.3. 14-[*N*-(Biotinyl)-12-aminododecanoxy]melampomagnolide B (4). To a solution of **6** (150 mg, 0.30 mmol) in DMF (2 mL), was added TBAF (1M in THF, 0.30 mL), and the resulting solution stirred at ambient temperature for 30 min. In another flask, biotin-pentafluorphenol (0.435 mg, 0.22 mmol) was dissolved in DMF (2 mL) and this solution was added to the flask containing **6**. The resulting solution was stirred for 12 h at room temperature and then evaporated to afford a sticky brown-colored gum. This residue was purified by silica gel column chromatography

to afford **4** (silica neutralized with Et_3N), CH_2Cl_2/*i*-PrOH, (67.0 mg), 45 % yield; white solid; 130−132 °C; ^{1}H NMR (300 MHz, $CDCl_3$) δ 6.27 (d, J = 3.3 Hz, 1H), 6.23(s, 1H), 5.98 (t, J = 5.5 Hz, 1H), 5.69 (t, J = 8.4 Hz, 1H), 5.55(d, J = 3.3 Hz, 1H), 5.40 (s, 1H), 4.65 (d, J = 12.6 Hz, 1H), 4.52 (m, 2H), 4.32 (m, 1H), 3.87 (t, J = 9.3 Hz, 1H), 3.23 (m, 3H), 2.92 (m, 3H), 2.75 (d, J = 15 Hz, 1H), 2.48–2.14 (m, 8H), 1.85−1.07 (m, 28H) 1.55 (s, 3H) ppm. ^{13}C NMR (75 MHz, $CDCl_3$) δ 173.5, 172.8, 169.4, 138.8, 135.0, 130.6, 120.4, 81.2, 66.7, 63.5, 61.9, 60.34, 60,2, 59.1, 55.5, 42.9, 40.8, 39.8, 36.8, 36.3, 34.5, 34.2, 32.2, 29.99, 29.90, 29.7, 29.6, 29.5, 29.4, 28.3, 27.2, 26.0, 25.8, 25.2, 24.8, 24.1, 18.3 ppm; ESI-MS *m/z*: 688 $(M+H)^+$; Anal. Calcd. for $C_{37}H_{57}N_3O_7S$: C, 64.60; H, 8.35; N, 6.11. Found C, 64.63; H, 8.24; N, 6.15.

6.2 Biological Assays

6.2.1. Streptavidin (SA) beads pull-down assay. Treated cells were washed three times in cold PBS and lysed in Buffer F (10mM Tris-HCl pH 7.5, 50mM NaCl, 30mM Sodium pyrophosphate, 50mM NaF, 5μM $ZnCl_2$, 1% Triton X-100) with freshly added proteinase inhibitors (1mM PMSF, 1XPIC, 0.1mM Na_3OV_4). Lysates were cleared by 10 mins of 12,000 rpm spinning at 4^o C and the supernatant was incubated with SA beads for 2 hours on an end-to-end rotor at 4^o C. Beads were then washed sequentially with 1XPBS, high salt wash buffer (500mM NaCl in 0.1M pH 5.0 NaOAc), low pH wash buffer (0.1M pH 2.8 glycine-HCl), and one last time in 1XPBS. After the wash steps, the SA beads were boiled for 10 mins in 2XSDS-PAGE sample buffer to elute down all pull-down products.

6.2.2. Immunobloting. Cell lysates or pull-down products were diluted in 5 x SDS-PAGE sample buffer (10% w/v SDS, 10mM DDT, 20% glycerol, 0.2M Tris-HCl, pH 6.8, 0.05% w/v bromophenol blue), and run on 8-10% SDS-PAGE gels. Protein gels were then transferred to PVDF membrane and blocked with 5% milk in 0.1% TBST (20 mM Tris-HCl pH 7.5, 137 mM NaCl, 0.1% Tween 20), followed by incubation with antibodies against p-p65(ser 536) (Cell Signaling), IKK-β (Cell Signaling), p65 (Santa Cruz), β-actin (Sigma), or SA-HRP probe (Thermo).

6.2.3. Cell Viability Assays. Cells treated with different concentrations of **1**, **3** or **4** were washed with cold PBS and resuspended in 200 μL of Annexin binding buffer (10 mM HEPES/NaOH pH 7.4; 140 mM NaCl; 2.5 mM $CaCl_2$). Annexin-V and 7-amino-actinomycin (7-AAD) were added and the tubes were incubated at ambient temperature in the dark for 15 mins. Cells were then diluted with 200 μL of Annexin binding buffer and analyzed immediately by flow cytometry. Viable cells were scored as Annexin V negative/7-AAD negative. Percent viability data provided are normalized to untreated control specimens.

Acknowledgements

This work was supported by grants from the Department of Defense (W81XWH-07-1-0601), and the New York State Stem Cell Foundation (C024964).

References

1. Skalska, J.; Brookes, P. S.; Nadtochiy, S. M.; Hilchey, S. P.; Jordan, C. T.; Guzman, M. L.; Maggirwar, S. B.; Briehl, M. M.; Bernstein, S. H. *PLoS ONE*, **2009**, *4*, e8115.
2. Bork, P. M.; Schmitz, M. L.; Kuhnt, M.; Escher, C.; Heinrich,M. *FEBS Lett*. **1997**, *402*, 85.
3. Wen, J.; You, K. R.; Lee, S. Y.; Song, C. H.; Kim, D. G. *J. Biol. Chem*., **2002**, *277*, 38954.
4. Hehner, S. P.; Heinrich, M.; Bork, P. M.; Vogt, M.; Ratter, F.; Lehmann, V.; Schulze-Osthoff, K.; Dröge, W.; Schmitz, M. L. *J. Biol. Chem*. **1998**, *273*, 1288.
5. Sweeney, C. J.; Li, L.; Shanmugam, R.; Bhat-Nakshatri, P. B.; Jayaprakasan, V.; Baldridge, L. A.; Gardner, T.; Smith, M.; Nakshatri, H.; Cheng, L. *Clin. Cancer Res*., **2004**, *10*, 5501.
6. Yip-Schneider, M. T.; Nakshatri, H.; Sweeney, C. J.; Marshall, M. S.; Wiebke, E. A.; Schmidt, C. M. Mol. *Cancer Ther*., **2005**, *4*, 587.
7. Nozaki, S.; Sledge, G. W.; Nakshatri, H. *Oncogene*, **2001**, *20*, 2178.
8. Guzman, M. L.; Rossi, R. M.; Karnischky, L.; Li, X.; Peterson, D. R.; Howard, D. S.; Jordan, C. T. *Blood*, **2005**, *105*, 4163.
9. Guzman, M. L.; Jordan, C. T. *Exp. Opin. Biol. Ther*., **2005**, *5*, 1147.
10. Neelakantan, S.; Nasim, S.; Guzman, M. L.; Jordan, C. T.; Crooks, P. A. *Bioorg. Med. Chem. Lett*., **2009**, *19*, 4346.
11. Nasim, S.; Crooks, P. A. *Bioorg. Med. Chem. Lett*., **2008**, *18*, 3870.
12. El-Feraly, F.S. *Phytochemistry*, **1984**, *23*, 2372.
13. Macias, F. A.; Galindo, J. C. G.; Guillermo, M. M. *Phytochemistry*, **1992**, *31*, 969.
14. Gonzalez, A.G.; Galindo, A.; Mar Afonso, M.; Mansilla, H.; Lopez, M. *Tetrahedron*, **1988**, *44*, 4585.
15. Kwok, B. H. B.; Koh, B.; Ndubuisi, M. I.; Elofsson, M.; Crews, C. M.; *Chem. Bio*., **2001**, *8*, 759.
16. Hehner, S.P.; Hofmann, T.G.; Droge, W.; Schmitz, M. L. *J. Immunol*. **1999**, *163*, 5617.